Drug Delivery

DOI: 10.1002/anie.201103806

Interlayer-Crosslinked Micelle with Partially Hydrated Core Showing Reduction and pH Dual Sensitivity for Pinpointed Intracellular Drug Release**

*Jian Dai, Shudong Lin, Du Cheng, Seyin Zou, and Xintao Shuai**

Although the utilization of polymeric micelles has demonstrated great potential in delivering anticancer drugs,[1,2] this technique is facing tremendous challenges. In particular, polymeric micelles usually show a drug-release profile that is not in favor of achieving optimal drug availability inside tumor cells. That is, a "burst release" of up to 20–30% of the encapsulated drug within several hours post micelle formation, followed by a slow diffusional drug release lasting for many days. The premature burst release leads to drug loss in micelle storage and blood circulation. Meanwhile, the second-stage slow drug release results in low intracellular drug availability insufficient for killing cancer cells. Therefore, development of delivery systems with better drug-release properties is still of great importance. One of the most promising strategies is to construct polymeric micelles that respond to specific stimulation, such as light exposure,[3] enzymatic degradation,[4] redox reaction,[5] or change in pH or temperature.[6–9]

Acid-triggered rapid release of drugs can be achieved inside tumor tissue (pH below 6.8) or lysosomal compartments (pH about 5.0) of cancer cells by using micelles of copolymers bearing pH-sensitive blocks, such as poly(L-histidine) and poly(β-amino ester).[6–8] Nevertheless, these pH-sensitive micelles were not designed to avoid the premature burst release of drugs. In addition, supramolecular nanoassemblies de-micellize when the polymer concentration drops below the critical micelle concentration (CMC), which is another underlying cause for the loss of drugs during blood circulation.

Recently, covalent crosslinking of the core or shell of self-assembled polymeric micelles has emerged as a viable strategy to prevent de-micellization-associated drug loss.[10,11] Among various approaches, the utilization of disulfide-containing reversible crosslinkers is of particular importance, owing to the fact that the disulfide bond is reducible and therefore can be cleaved by glutathione (GSH), a thiol-containing oligopeptide predominantly found inside cells (up to the millimolar scale). Indeed, shell-crosslinked micelles (SCMs) obtained using disulfide-containing agents have demonstrated great potential for specifically releasing the loaded cargos inside cells.[12,13] In spite of their potential in reducing premature drug leakage, these SCMs cannot rapidly release drugs inside cells because drug release from their nonsensitive cores still follows a diffusion-controlled mechanism.

Herein, we describe the first example of a highly packed interlayer-crosslinked micelle (HP-ICM) with reduction and pH dual sensitivity, which comprises a polyethylene glycol (PEG) corona to stabilize the particles, a highly compressed pH-sensitive partially hydrated core to load anticancer drugs, and a disulfide-crosslinked interlayer to tie up the core against expansion at neutral pH. The HP-ICM was stable and drug leakage free in a neutral pH environment without reducing agent. However, when the HP-ICM was internalized into cells and trapped inside lysosomes featuring low pH ($\approx$5) and enriched reducing agent (GSH), the pH-sensitive core was unpacked and thus erupted to burst release the anticancer drug (Figure 1).

The reduction- and pH-sensitive interlayer-crosslinked micelle with partially hydrated core was prepared from a triblock copolymer of monomethoxy polyethylene glycol (mPEG), 2-mercaptoethylamine (MEA)-grafted poly(L-aspartic acid) (PAsp(MEA)), and 2-(diisopropylamino)ethylamine (DIP)-grafted poly(L-aspartic acid) (PAsp(DIP)). The copolymer was synthesized by ring-opening polymerization of β-benzyl L-aspartate *N*-carboxy-anhydride (BLA-NCA) in combination with click and aminolysis reactions (see the Supporting Information, Figure S1). So far, most reported shell-crosslinked nanoparticles have been based on polyacrylate or polyacrylamide.[11,14] We chose biodegradable polypeptide as the copolymer backbone in consideration of biocompatibility requirements in drug delivery. Poly(BLA) aminolysis with MEA and DIP introduced the crosslinkable thiol and pH-sensitive tertiary amino groups onto the middle and end blocks of the copolymer, respectively.[15–17]

NMR and FTIR analyses confirmed the chemical structures of the polymers (see the Supporting Information, Figures S3–S6). Gel permeation chromatography measurements also evidenced the successful synthesis of mPEG-

[*] Dr. J. Dai,[+] S. Lin,[+] Dr. D. Cheng, Prof. X. Shuai
PCFM Lab of Ministry of Education, School of Chemistry and Chemical Engineering
Sun Yat-sen University, Guangzhou 510275 (China)
E-mail: shuaixt@mail.sysu.edu.cn
S. Zou, Prof. X. Shuai
Center of Biomedical Engineering, Zhongshan School of Medicine
Sun Yat-sen University, Guangzhou 510275 (China)
[+] These authors contributed equally to this work.

[**] This research was supported by the Natural Science Foundation of China (50830107, 20974129, U1032002) and Guangdong (9351027501000003), the 863 Programs (2009AA03Z310) and Projects for the Creation of Significant New Drugs Programs (2009ZX09501-023) of the Ministry of Science and Technology of China.

Supporting information for this article is available on the WWW under http://dx.doi.org/10.1002/anie.201103806.

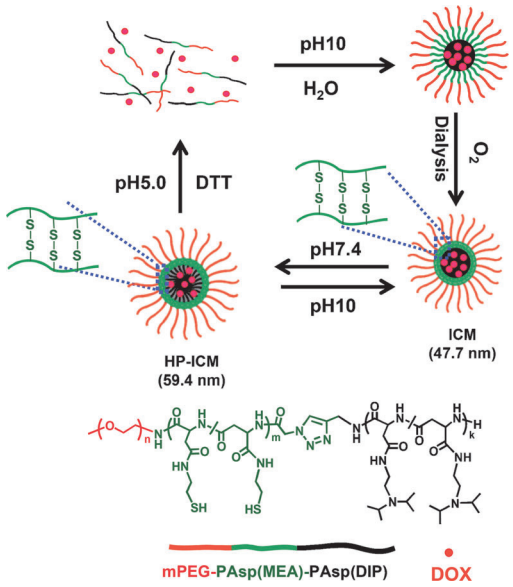

Figure 1. Formation and structural transitions of the dual-sensitive HP-ICM. Polymer composition based on ^{1}H NMR spectroscopy: $n = 45$, $m = 15$, $k = 14$. DOX = doxorubicin.

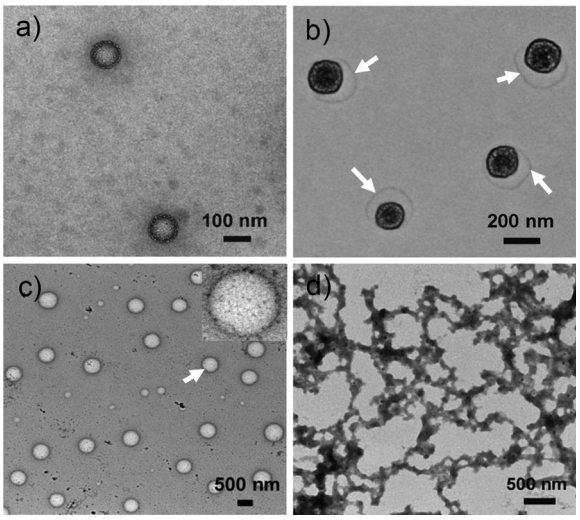

Figure 2. Transmission electron microscopy (TEM) images of the nanoassembly at pH values of a) 7.4, b) 5.0, c) 7.4 with addition of DTT, and d) 5.0 with addition of DTT. The HP-ICMs shown in (a) were decorated with Au. In TEM measurements, the Au-decorated HP-ICMs were not stained and other samples were stained with uranyl acetate. The arrows in (b) indicate the "watermark" of staining agent formed as a result of nanocage shrinkage in sample drying. DTT concentration (if added): 10 mM.

Table 1: Size change of the nanoassembly measured by DLS; size was undetectable at pH 5.0 with addition of DTT (10 mM).

	ICM pH 10	HP-ICM pH 7.4	Au-HP-ICM pH 7.4	Nanocage pH 5.0	Swollen micelle pH 7.4 + DTT
Size [nm]	47.7 ± 3	59.4 ± 5	103.6 ± 10	269.6 ± 40	546.2 ± 45

PAsp(MEA)-PAsp(DIP) (see the Supporting Information, Figure S7). The copolymer has a composition of 2 kDa for mPEG, 2.7 kDa for PAsp(MEA), and 3.3 kDa for PAsp(DIP). By acid–base titration, we determined that the protonation degrees of the DIP tertiary amino groups of mPEG-PAsp-(MEA)-PAsp(DIP) were 100, 41.46, and 0% at pH 5.0, 7.4, and 10, respectively, which is in line with a previous report that the DIP group of PAsp(DIP) was partially protonated at pH 7.4.[18]

The dual-sensitive HP-ICM was prepared by self-assembly of the copolymer at pH 10, followed by interlayer crosslinking upon disulfide formation and then adjusting the pH of the solution to 7.4 (Figure 1, Table 1). The approach featured the formation of the small ICM first and then the generation of a tight package around the core, which constrained the particle expansion when the core underwent a pH-inducible "dehydration–partial hydration" transition to form the HP-ICM (see the Supporting Information, Figure S2). Raman spectral measurement demonstrated disulfide formation (see the Supporting Information, Figure S8). Furthermore, a considerably high degree of crosslinking, that is, 88.5% conversion of thiol to disulfide, was achieved according to the measurement of sulfhydryl content using Ellman's reagent.[19] The anticancer drug doxorubicin (DOX) was encapsulated in the HP-ICM core at a relatively high loading content (10.5%).

Dynamic light scattering (DLS), TEM, and ^{1}H NMR studies provided strong evidence that the prepared HP-ICM possessed pH and reduction dual sensitivity (Figure 2). Since the DIP groups of PAsp(DIP) were completely deprotonated at pH 10, the nanoassembly at pH 10 should possess a micelle structure with a compact core of self-assembled hydrophobic PAsp(DIP) chains, which explains the small hydrodynamic size (47.7 nm) of the ICMs at pH 10 (Table 1). When the solution was adjusted to pH 7.4, the average hydrodynamic size of the nanoassembly was merely increased to 59.4 nm. Based on the fact that the DIP groups of mPEG-PAsp-(MEA)-PAsp(DIP) were partially protonated at pH 7.4, the nanoassembly core should be partially hydrated at this pH (see the Supporting Information, Figure S2).

Moreover, the very slight particle expansion (59.4 vs. 47.7 nm) accompanying the solution pH change from 10 to 7.4 and the significant size increase of nanoparticles (546.2 vs. 59.4 nm) upon adding dithiothreitol (DTT, 10 mM) to the solution at pH 7.4 strongly indicated that the interlayer-crosslinked nanoassembly at pH 7.4 without addition of DTT was highly packed (Table 1). In other words, the crosslinked PAsp(MEA) interlayer had significantly constrained the HP-ICM core against further expansion at pH 7.4. Obviously, when DTT (10 mM) was added to the solution at pH 7.4, the HP-ICM was turned into a highly "swollen" micelle, the partially solvated PAsp(DIP) core of which was much more expanded upon unpacking the tight enclosure of the crosslinked interlayer (Figure 2c).

The PAsp(MEA) interlayer of the small-sized HP-ICM was decorated with gold nanoparticles (ca. 1 nm) to enhance the shell rigidity for high-resolution TEM imaging.[20–22] The contrast between the core and shell was enhanced by the settlement of the Au dots in the shell, and the TEM observations clearly showed that the HP-ICM possessed a

spherical core–shell structure (Figure 2a). It was noted that loading of gold nanoparticles into the shell led to a size increase to 103.6 nm from 59.4 nm. Most likely, a rigid gold layer made the shell more extended. Furthermore, reaction between the disulfide bonds and gold nanoparticles may decrease the package tightness against core expansion. The HP-ICM was turned into a nanocage structure at pH 5.0 without adding DTT (Figure 2b).

The particle size of the nanocages detected by TEM (ca. 200 nm) was smaller than that determined by DLS (269.6 nm) because of the shrinkage of hollow nanoparticles during the sample drying process, as evidenced by the clear "watermark" of the staining agent asymmetrically surrounding the nanoparticles. In this case, the DIP groups of mPEG-PAsp(MEA)-PAsp(DIP) were fully protonated and thus the HP-ICM core was completely dissolved (Figure 2b). Consequently, the crosslinked interlayer could no longer provide enough strength to counteract the enhanced force for further core expansion resulting from PAsp(DIP) chain dissolution and electrostatic repulsion of more protonated DIP groups. As a result, the nanocage was much bigger than the HP-ICM (269.6 vs. 59.4 nm; Figure 2b, Table 1). Finally, when DTT (10 mM) was added to the pH 5.0 solution, disassembly of the HP-ICM was detected in DLS and TEM measurements, which indicated that the disulfide crosslinking was broken and the polymer chains were completely dissolved. Therefore, drying the solution led to the formation of random polymeric aggregates (Figure 2d). ^{1}H NMR analysis in D_2O further evidenced the structural transitions of the HP-ICM under different conditions (see the Supporting Information, Figure S10).

The DOX fluorescence intensity of the HP-ICM solution at pH 7.4 without adding DTT was very weak, whereas it was significantly intensified upon single stimulation by either decreasing the solution pH to 5.0 or adding reducing agent GSH or DTT (see the Supporting Information, Figure S11). Moreover, the highest DOX fluorescence intensity was detected when dual stimuli (pH 5.0 and addition of DTT) were applied. Consistent results were obtained in the quantitative determination of drug release by measuring the UV/Vis absorbance intensity of DOX outside dialysis tubes (Figure 3a and the Supporting Information, Figure S12).[23] Notably, DOX release at neutral pH without adding DTT was hardly detected. When 10 μM GSH or DTT existed in the neutral solution, only a very slow DOX release was detected, as also determined in other types of shell disulfide-crosslinked micelles.[13] These results imply that DOX leakage from the HP-ICM may be significantly reduced during sample storage (no reductant) and blood circulation (ca. 10 μM GSH).

Although significant acceleration of DOX release was observed upon either adding 10 mM GSH/DTT or adjusting the pH to 5.0, the most rapid release was determined when dual stimuli were applied simultaneously. In the latter case, about 95% of DOX was released within just 5 h. Since the experimental conditions mimicked the environment inside lysosomes, that is, pH around 5.0 and existence of about 10 mM GSH, our results imply that the HP-ICM may rapidly release the cargo after entering cancer cells through endocytosis and being trapped inside lysosomes. Moreover, the dual-

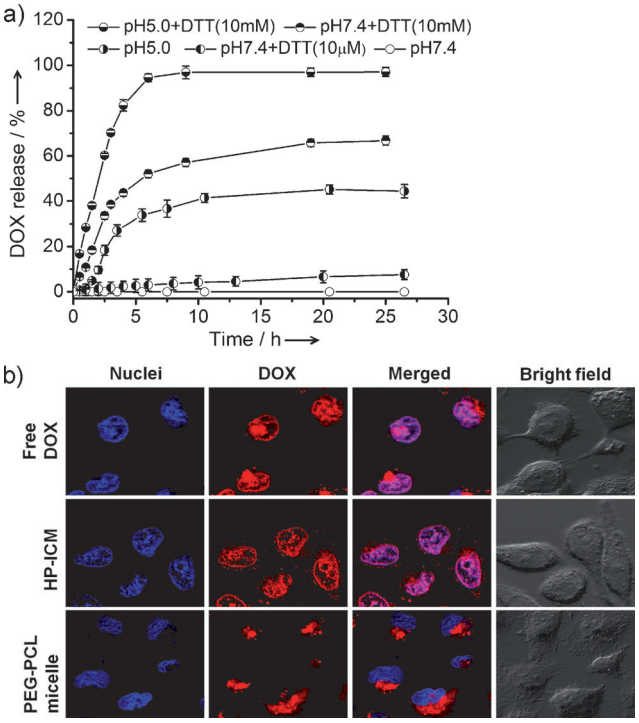

Figure 3. a) Quantitative DOX release from the dual-sensitive HP-ICM (mean ± standard deviation (SD), $n = 3$). b) Intracellular DOX release and migration into nuclei observed by confocal laser scanning microscopy (CLSM). Bel-7402 cells were incubated (37 °C) for 6 h at a DOX-equivalent dosage of 10 μg per dish. DOX loading contents: 10.5% in HP-ICMs and 5.1% in PEG2k-PCL3k micelles. Nuclei were stained with Hoechst 33342 (blue).

sensitive DOX release phenomenon can be well explained based on the structural transitions of HP-ICM (see the Supporting Information, Figure S2). When DOX molecules were embedded at relatively high density in the compact PAsp(DIP) matrix of the HP-ICM core, there was a fluorescence quenching effect.[15] However, when the HP-ICM was transformed to a highly swollen micelle or nanocage, DOX diffused out of the nanocarrier much more easily. More importantly, when dual stimuli were applied, dissociation of the nanoassembly was triggered, which resulted in the most rapid release of DOX.

As nanoparticles are eventually trapped inside lysosomes after endocytosis, rapid lysosomal drug release is crucial for an ideal therapeutic effect. Therefore, the intracellular release of DOX from the HP-ICM in human hepatoma Bel-7402 and ovarian cancer SKOV-3 cells was investigated. It is well known that free DOX quickly enters nuclei after cell uptake,[24] whereas DOX transported by nonsensitive micelles accumulates in nuclei very slowly.[25] Therefore, free DOX and DOX-loaded nonsensitive micelles [(41.0 ± 0.7) nm; DOX content: 5.1%] based on the diblock copolymer of PEG and poly(ε-caprolactone) (PCL), that is, PEG2k-PCL3k, were employed as positive and negative controls, respectively. As shown in Figure 3b, fast accumulation of DOX in nuclei of Bel-7402 cells was observed for free DOX and DOX-loaded HP-ICMs. After 6 h of cell incubation, strong red fluorescence of DOX was observed in nuclei, which were even

turned pink in the merged fluorescence images as a result of the overlapping fluorescence of Hoechst 33342 and DOX. On the contrary, DOX fluorescence was observed mainly in cytoplasm for the nonsensitive PEG-PCL micelle. The same results were obtained in SKOV-3 cells (see the Supporting Information, Figure S13). The rapid release of DOX from the HP-ICMs inside cells was consistent with the data obtained in buffered solutions (Figure 3a). Based on these results, the low pH value and reducing agent GSH inside lysosomes should have caused disassembly of the dual-sensitive HP-ICMs, thereby resulting in the rapid lysosomal release and nucleic accumulation of DOX.

Further anticancer studies verified the importance of the low pH and reduction co-triggered rapid release of DOX. The copolymer showed very low cytotoxicity even at fairly high concentrations up to 70–100 $\mu g\,mL^{-1}$ (see the Supporting Information, Figure S14). DOX transported by the dual-sensitive HP-ICM appeared much more cytotoxic than that transported by the PEG-PCL micelle, and approached the cytotoxicity of free DOX in both Bel-7402 and SKOV-3 cells (see the Supporting Information, Figure S14). The intrinsic fluorescence of DOX enabled direct tracking of the DOX-loaded HP-ICMs after intravenous injection into nude mice bearing the Bel-7402 xenograft. Accumulation of HP-ICMs at the tumor site depending on postinjection time was detected (Figure 4a). Ex vivo imaging of organs of interest showed distribution of the DOX-loaded HP-ICMs in comparison with PEG-PCL micelles (see the Supporting Information, Figure S15). The results are supportive of reduced drug release from HP-ICMs in blood circulation, and are in line with the previous report that nanoparticles with similar small sizes (60–70 nm) accumulated preferentially in tumors through the enhanced permeability and retention (EPR) effect and at the reticuloendothelial sites such as liver.[26]

Measurements on tumor size (Figure 4b), body weight, and survival rate (see the Supporting Information, Figure S16) demonstrated that treatment using the DOX-loaded dual-sensitive HP-ICM resulted in the best therapeutic effect. Even though the DOX-loaded HP-ICM was somewhat less cytotoxic than free DOX in vitro (see the Supporting Information, Figure S14), its performance was better than that of free DOX in vivo. When the DOX-loaded dual-sensitive HP-ICM was administered, terminal deoxynucleotidyl transferase-mediated dUTP nick-end labeling (TUNEL) analysis detected the highest level of cell apoptosis in tumor tissue. Meanwhile, the level of cleaved caspase-3 protein, a key molecular indicator for cells under the apoptotic pathway, was significantly elevated. The fewest tumor cells were shown in hematoxylin and eosin (H&E) staining as well (Figure 4c).

In summary, we have developed a highly packed interlayer-crosslinked micelle with partially hydrated core (HP-ICM) for intracellular drug release. The novel HP-ICM with pH and reduction dual sensitivity was formed based on a well-defined copolymer mPEG-PAsp(MEA)-PAsp(DIP). Drug leakage can be avoided in micelle storage and significantly reduced in blood circulation, whereas a burst release of drug was triggered in an acidic and reductant-enriched environment such as in lysosomes. Since drug leakage in sample storage or blood circulation and slow drug release inside cancer cells are two great challenges for conventional nanocarriers at present, the dual-sensitive drug release property of our HP-ICM is very meaningful. Cell and animal studies revealed the great potential of the dual-sensitive HP-ICM for achieving an optimal therapeutic effect of the transported drugs in cancer treatment.

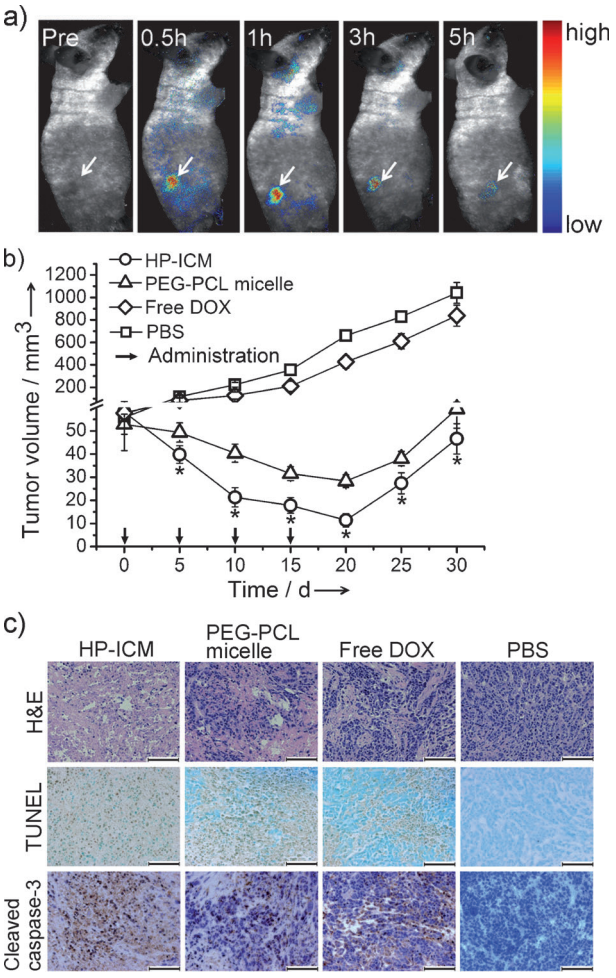

Figure 4. a) In vivo DOX fluorescence images showing passive tumor accumulation of DOX-loaded HP-ICMs after tail-vein injection into nude mice bearing the Bel-7402 xenograft (dose: 5 mg DOX per kg body weight). b) Tumor growth inhibition in nude mice bearing the Bel-7402 tumor after tail-vein injection of different formulations ($n = 20$; dose: 5 mg DOX per kg body weight per injection for DOX or DOX-loaded micelles). c) Ex vivo histological and immunohistochemical analyses of Bel-7402 tumor sections (30 days after the first treatment). Nuclei were stained blue while extracellular matrix and cytoplasm were stained red in H&E staining. Brown and green stains indicated apoptotic and normal cells, respectively, in TUNEL analysis; brown and blue stains indicated cleaved caspase-3 protein and nuclei, respectively, in immunohistochemical assay. Scale bars in (c): 100 μm. The values in (b) are mean ± SD. $^*p < 0.01$ versus PEG-PCL micelle (*t*-test using SPSS, 13.0).

Received: June 4, 2011
Revised: July 22, 2011
Published online: September 5, 2011

Keywords: acidity · antitumor agents · drug delivery · micelles · reduction

[1] J. H. Park, S. Lee, J. H. Kim, K. Park, K. Kim, I. C. Kwon, *Prog. Polym. Sci.* **2008**, *33*, 113 – 137.
[2] K. Miyata, R. J. Christie, K. Kataoka, *React. Funct. Polym.* **2011**, *71*, 227 – 234.
[3] H. I. Lee, W. Wu, J. K. Oh, L. Mueller, G. Sherwood, L. Peteanu, T. Kowalewski, K. Matyjaszewski, *Angew. Chem.* **2007**, *119*, 2505 – 2509; *Angew. Chem. Int. Ed.* **2007**, *46*, 2453 – 2457.
[4] C. Wang, Q. S. Chen, Z. Q. Wang, X. Zhang, *Angew. Chem.* **2010**, *122*, 8794 – 8797; *Angew. Chem. Int. Ed.* **2010**, *49*, 8612 – 8615.
[5] N. Ma, Y. Li, H. P. Xu, Z. Q. Wang, X. Zhang, *J. Am. Chem. Soc.* **2010**, *132*, 442 – 443.
[6] E. S. Lee, K. T. Oh, D. Kim, Y. S. Youn, Y. H. Bae, *J. Controlled Release* **2007**, *123*, 19 – 26.
[7] H. Yin, E. S. Lee, D. Kim, K. H. Lee, K. T. Oh, Y. H. Bae, *J. Controlled Release* **2008**, *126*, 130 – 138.
[8] X. L. Wu, J. H. Kim, H. Koo, S. M. Bae, H. Shin, M. S. Kim, B. H. Lee, R. W. Park, I. S. Kim, K. Choi, I. C. Kwon, K. Kim, D. S. Lee, *Bioconjugate Chem.* **2010**, *21*, 208 – 213.
[9] Y. J. Jun, U. S. Toti, H. Y. Kim, J. Y. Yu, B. Jeong, M. J. Jun, Y. S. Sohn, *Angew. Chem.* **2006**, *118*, 6319 – 6322; *Angew. Chem. Int. Ed.* **2006**, *45*, 6173 – 6176.
[10] X. Shuai, T. Merdan, T. Kissel, *Bioconjugate Chem.* **2004**, *15*, 441 – 448.
[11] E. S. Read, S. P. Armes, *Chem. Commun.* **2007**, 3021 – 3035.
[12] Y. Li, B. S. Lokitz, S. P. Armes, C. L. McCormick, *Macromolecules* **2006**, *39*, 2726 – 2728.
[13] A. N. Koo, H. J. Lee, S. E. Kim, J. H. Chang, C. Park, C. Kim, J. H. Park, S. C Lee, *Chem. Commun.* **2008**, 6570 – 6572.
[14] R. K. O'Reilly, C. J. Hawker, K. L. Wooley, *Chem. Soc. Rev.* **2006**, *35*, 1068 – 1083.
[15] K. Zhou, Y. Wang, X. Huang, K. Luby-Phelps, B. D. Sumer, J. Gao, *Angew. Chem.* **2011**, *123*, 6233 – 6238; *Angew. Chem. Int. Ed.* **2011**, *50*, 6109 – 6114.
[16] J. Du, Y. Tang, A. L. Lewis, S. P. Armes, *J. Am. Chem. Soc.* **2005**, *127*, 17982 – 17983.
[17] Y. Lee, S. Fukushima, Y. Bae, S. Hiki, T. Ishii, K. Kataoka, *J. Am. Chem. Soc.* **2007**, *129*, 5362 – 5363.
[18] M. Nakanishi, J. S. Park, W. D. Jang, M. Oba, K. Kataoka, *React. Funct. Polym.* **2007**, *67*, 1361 – 1372.
[19] R. J. Verheul, S. van der Wal, W. E. Hennink, *Biomacromolecules* **2010**, *11*, 1965 – 1971.
[20] S. I. Tanaka, J. Miyazaki, D. K. Tiwari, T. Jin, Y. Inoue, *Angew. Chem.* **2011**, *123*, 451 – 455; *Angew. Chem. Int. Ed.* **2011**, *50*, 431 – 435.
[21] X. Chen, Y. An, D. Zhao, Z. He, Y. Zhang, J. Cheng, L. Shi, *Langmuir* **2008**, *24*, 8198 – 8204.
[22] M. A. Nash, J. J. Lai, A. S. Hoffman, P. Yager, P. S. Stayton, *Nano Lett.* **2010**, *10*, 85 – 91.
[23] N. Cao, D. Cheng, S. Zou, H. Ai, J. Gao, X. Shuai, *Biomaterials* **2011**, *32*, 2222 – 2232.
[24] N. Nasongkla, E. Bey, J. Ren, H. Ai, C. Khemtong, J. S. Guthi, S. F. Chin, A. D. Sherry, D. A. Boothman, J. Gao, *Nano Lett.* **2006**, *6*, 2427 – 2430.
[25] X. Shuai, H. Ai, N. Nasongkla, S. Kim, J. Gao, *J. Controlled Release* **2004**, *98*, 415 – 426.
[26] J. H. Park, G. V. Maltzahn, E. Ruoslahti, S. N. Bhatia, M. J. Sailor, *Angew. Chem.* **2008**, *120*, 7394 – 7398; *Angew. Chem. Int. Ed.* **2008**, *47*, 7284 – 7288.

